Dissection of Genomewide-Scan Data in Extended Families Reveals a Major Locus and Oligogenic Susceptibility for Age-Related Macular Degeneration

Sudha K. Iyengar,[1] Danhong Song,[1] Barbara E. K. Klein,[2] Ronald Klein,[2] James H. Schick,[1] Jennifer Humphrey,[1] Christopher Millard,[1] Rachel Liptak,[1] Karlie Russo,[1] Gyungah Jun,[1] Kristine E. Lee,[2] Bonnie Fijal,[1] and Robert C. Elston[1]

[1]Department of Epidemiology and Biostatistics, Case Western Reserve University, Cleveland, OH; and [2]Department of Ophthalmology and Visual Sciences, University of Wisconsin Medical School, Madison, WI

To examine the genetic basis of age-related macular degeneration (ARMD), a degenerative disease of the retinal pigment epithelium and neurosensory retina, we conducted a genomewide scan in 34 extended families (297 individuals, 349 sib pairs) ascertained through index cases with neovascular disease or geographic atrophy. Family and medical history was obtained from index cases and family members. Fundus photographs were taken of all participating family members, and these were graded for severity by use of a quantitative scale. Model-free linkage analysis was performed, and tests of heterogeneity and epistasis were conducted. We have evidence of a major locus on chromosome 15q (GATA50C03 multipoint $P = 1.98 \times 10^{-7}$; empirical $P \leq 1.0 \times 10^{-5}$; single-point $P = 3.6 \times 10^{-7}$). This locus was present as a weak linkage signal in our previous genome scan for ARMD, in the Beaver Dam Eye Study sample (D15S659, multipoint $P = .047$), but is otherwise novel. In this genome scan, we observed a total of 13 regions on 11 chromosomes (1q31, 2p21, 4p16, 5q34, 9p24, 9q31, 10q26, 12q13, 12q23, 15q21, 16p12, 18p11, and 20q13), with a nominal multipoint significance level of $P \leq .01$ or LOD ≥ 1.18. Family-by-family analysis of the data, performed using model-free linkage methods, suggests that there is evidence of heterogeneity in these families. For example, a single family (family 460) individually shows linkage evidence at 8 loci, at the level of $P < .0001$. We conducted tests for heterogeneity, which suggest that ARMD susceptibility loci on chromosomes 9p24, 10q26, and 15q21 are not present in all families. We tested for mutations in linked families and examined SNPs in two candidate genes, hemicentin-1 and EFEMP1, in subsamples (145 and 189 sib pairs, respectively) of the data. Mutations were not observed in any of the 11 exons of EFEMP1 nor in exon 104 of hemicentin-1. The SNP analysis for hemicentin-1 on 1q31 suggests that variants within or in very close proximity to this gene cause ARMD pathogenesis. In summary, we have evidence for a major ARMD locus on 15q21, which, coupled with numerous other loci segregating in these families, suggests complex oligogenic patterns of inheritance for ARMD.

Introduction

Age-related macular degeneration (ARMD) is the most common cause of severe visual disability and blindness in the United States and other developed countries (Jonasson and Thordarson 1987; Vinding 1990; Klein et al. 1992; Balatsoukas et al. 1995; Attebo et al. 1996; Evans and Wormald 1996; VanNewkirk et al. 2000; Buch et al. 2001; VanNewkirk et al. 2001; Harvey 2003). The

prevalence of ARMD in the population aged >65 years is 9% and reaches 28% in those aged >75 years (Klein et al. 1992, 1997, 1999). Early ARMD is manifested by large soft drusen, with progression to either geographic atrophy or neovascularization in late ARMD. The atrophic form involves modifications in pigment distribution, loss of retinal pigment epithelium [RPE] cells and photoreceptors, and reduced retinal function due to an overall atrophy of the cells. The prominent features of the neovascular form of ARMD involve proliferation of abnormal choroidal vessels, which enter the Bruch's membrane and RPE layer into the subretinal space, thereby resulting in detachments of the sensory retina or RPE, hemorrhage, exudates and glial proliferation with scarring. The molecular basis of this disease is not known and the presence of specific lesions described above are used to characterize its presence and severity and to tailor treatment for advanced stages of the dis-

ease. Antioxidants and vitamin supplements have been shown to lower the incidence of progression to late stages of ARMD from 29% to 21% (Anonymous 2001). Established treatment options for the neovascular forms of the disease, photocoagulation and photodynamic therapy, have also been shown to have some benefit to a limited number of persons with this condition (Bressler 2002; Hunt and Margaron 2003; Mittra 2003). A significant number of persons with this condition, despite available interventions, will progress to severe visual loss. Understanding the pathophysiology of this disease should aid in designing more universal and effective treatment.

Risk for ARMD development is associated with numerous environmental factors, such as smoking (Klein et al. 1993, 1998b, 2002b; DeBlack 2003), sunlight exposure (Cruickshanks et al. 1993), and diet (Seddon et al. 1994; Mares-Perlman et al. 1996; Vanden-Langenberg et al. 1998; Jacques 1999; Anonymous 2002). Observational studies of these risk factors have not given consistent results; nor do they fully explain the excessive familial clustering of ARMD. Several lines of evidence have convincingly established the importance of genetic factors in the etiology of ARMD, including twin (Hammond et al. 2002) and family studies (Keverline et al. 1998; Yoshida et al. 2000; Stone et al. 2001), population-based genetic epidemiologic studies (Klein et al. 2001a), and segregation analyses (Heiba et al. 1994). Comparison of casewise concordance in 226 MZ and 280 DZ twin pairs showed higher concordance rates among MZ (0.37) versus DZ (0.19) twins (Hammond et al. 2002). Examination of sibling correlations for ARMD quantitative scores in 564 sibships in the Beaver Dam Eye study (Heiba et al. 1994) showed significant correlations. Further modeling and parameter fitting suggested that single major gene segregation could explain 89%–97% of the genetic variability or 55%–57% of the total variability.

A number of genes implicated in other morphologically distinct forms of macular degeneration (Allikmets 1997b; De La Paz et al. 1997; Rivera et al. 2000; Gorin 2001; Guymer et al. 2001, 2002; Bernstein et al. 2002) have been investigated in ARMD, but no consistent associations have emerged. More recently, several genomewide scans (Klein et al. 1998a; Weeks et al. 2000; Weeks et al. 2001; Majewski et al. 2003; Schick et al. 2003) for ARMD have been conducted and analyzed using both model-free and model-based linkage methods. Novel ARMD loci on chromosomes 1q31, 3p13, 4q32, 9q33, 10q26, 12q23, and 17q25 were identified in these scans. The loci on chromosomes 1q31 and 10q26 were observed in independent scans (Klein et al. 1998a; Weeks et al. 2001; Majewski et al. 2003) and are the only loci that have been validated, thus far, for ARMD. On the basis of these results, it is apparent that the phenotypic and genetic heterogeneity of ARMD is complex.

To further comprehend the genetic basis of ARMD, we have undertaken a genome scan of extended families identified from the Retinal Clinic at the University of Wisconsin. In contrast to our previous genome scan (Schick et al. 2003), which was performed on a sample of small families from Beaver Dam, WI, with all grades of ARMD from early to late but with a small bias towards higher grades, the families in this second sample (FARMS, for "Family ARM Study") were larger and were ascertained through probands with severe ARMD. To fully utilize the data available, analysis was performed on a quantitative scoring system that represents the full spectrum of severity of ARMD lesions. Compared with assignment of binary affection status based on clinical criteria or a threshold value, use of quantitative scores reduces the corresponding probability of misclassification of individuals and may provide increased power to detect linkage signals. Although the data could be dichotomized for analysis, for comparison with previous analyses of ARMD, no single dichotomy would correspond to all such previous analyses. In regions that gave evidence suggestive of linkage, we analyzed candidate genes that have been associated elsewhere with other forms of macular degeneration.

Subjects, Material, and Methods

Subject Recruitment and Evaluation

Families.—Thirty-four index cases and their families, visiting the Retinal Clinic at the University of Wisconsin, were invited to participate in a study of genetic correlates for ARMD. The index cases were people with advanced ARMD. All consenting subjects and family members were interviewed using a uniform interview schedule and had fundus photographs taken. Family members who lived at remote sites were sent to local clinics for blood draws and photographs. Fundus photographs were graded using a codified grading scheme that is briefly described below. The protocol for phlebotomy and subject testing was approved by the Institutional Review Board at the University of Wisconsin.

Phenotypic evaluation.—Stereoscopic photographs of the retina were graded using standardized protocols to detect and classify the presence and severity of ARM lesions (Klein and Klein 1991; Bird et al. 1995; Klein et al. 1991a, 1991b, 1991c, 1997). Details of the grading procedure have been described elsewhere (Klein et al. 1991a, 1991b).

Two gradings were performed for each eye (Klein and Klein 1991, 1995; Klein et al. 1991a, 1991b, 1992, 1997, 2001b, 2002a). First, a preliminary masked grading was done by one of two senior graders. Next, de-

tailed gradings were performed by one of three other experienced graders. For detailed grading, each eye was graded independently of the other. The assessment consisted of a subfield-by-subfield, lesion-by-lesion, evaluation of each photograph set using the Wisconsin Age-Related Maculopathy Grading System (Klein et al. 1991*a*, 1991*b*). Next, a series of edits and reviews was performed. Standardized edit rules were used to adjudicate disagreements (Klein et al. 1991*a*, 1997).

A 16-level (0–15) severity scale based on drusen size, type, and area; pigmentary abnormalities; geographic atrophy; and signs of exudative macular degeneration was constructed. The ordering of the scale was based on associations of the presence and absence of early signs of age-related maculopathy with the incidence of geographic atrophy or exudative macular degeneration (Klein and Klein 1995).

An average score was calculated from scores of both eyes. However, if a score was missing for either eye, the score for the available eye was substituted for the missing score (this occurred for 2.42% of the subjects participating in the study). We used multiple regression analysis to investigate the effects of age, age^2, smoking, and sex, along with their interactions. As a result, we found that age and age^2 were the only significant terms in the variation of the maculopathy in this sample, assuming independence among subjects. We first calculated residuals from the regression model, as follows: $\text{ARMD}_{\text{residual}} = (\text{ARMD}_{\text{left eye}} + \text{ARMD}_{\text{right eye}})/2 - 13.62391 + 0.51210 \times \text{age} - 0.00581 \times \text{age}^2$. These residuals were utilized as indicated below in the linkage analysis.

Molecular Methods

Genome scan. — High molecular weight DNA was isolated from buffy coats (Miller et al. 1988) and 381 markers on 22 autosomes were genotyped in 349 sib pairs from 34 extended families. We used the Weber Set 10 microsatellite marker set, which has an average marker spacing of 8.85 Kosambi cM. Two additional markers, D1S406 and D1S236, in close proximity to the ABCA4 (retina-specific ABC transporter) gene were also genotyped. This gene is mutated in one form of Stargardt disease (STGD) and was hypothesized to be a candidate gene for ARMD (Allikmets et al. 1997*a*, 1997*b*; Allikmets 2000).

After extracting DNA from the blood samples, we used a fluorescence-based genotyping method for the genome scan. PCR primers conjugated with fluorescent dyes were purchased from IDT technology and Applied Biosystems. Genomic DNA (at 10 ng/μl, 3 μl) was PCR amplified using 0.225 U Platinum *Taq* DNA Polymerase (Gibco), Tris-HCl (200 mM, pH 8.4), dNTPs (200 μM each), MgCl$_2$ (1.0–3.0 mM), and forward and reverse

PCR primers (0.2 μM). The final reaction volume was 12 μl and the reactions were carried out in 96-well plates on an MJ Research Tetrad DNA Engine. The amplification reactions were optimized for the fluorescent dye-labeled primers, using the published conditions as the initial value. Eight to 10 markers were pooled after PCR, to create multiplexed panels. The multiplexed markers were run on an ABI 3700 capillary machine (Applied Biosystems). Five percent of the sample were blindly replicated, and two Centre d'Etude du Polymorphisme Humain (CEPH) controls were also included on each gel, to serve as internal controls. The ABI ROX 500 standard (present in every lane) was used to estimate the size of alleles.

Fine mapping. — After reviewing the initial outcome of the genome scan, regions on chromosomes 1q, 12q, and 15q that showed interesting results were followed up by typing additional markers. Thus, 4 markers on chromosome 1, 25 markers on chromosome 12, and 14 markers on chromosome 15 were also genotyped, decreasing the average intermarker distance at these locations to 3.13, 3.40, and 2.86 cM, respectively. The markers on chromosome 1q21-35—D1S466, D1S202, D1S2625, and D1S413—covered a 26-cM region previously linked to an autosomal dominant locus for a dry type of ARM (Klein et al. 1998*a*). The region on chromosome 12q was in close proximity to the linkage signal in our prior genome scan (Schick et al. 2003).

Molecular analyses of candidate genes. — As described in the "Statistical Methods" section that follows, we performed model-free linkage analyses of all the families jointly to identify regions with *P* values <.01, followed by individual analysis of the larger families to determine which families contributed to particular linkage signals. On the basis of these analyses, we identified three families contributing to the chromosome 1q signal and three families contributing to a chromosome 2p signal. Candidate genes hemicentin-1 (Ensembl transcript ID ENSG00000143341) and EGF-containing fibulin-like extracellular matrix protein 1 (EFEMP1 [MIM 601548]) on chromosomes 1q31 and 2p16, mutated in a dry form of ARM (Klein et al. 1998*a*; Schultz et al. 2003) and in Malattia Leventinese and Doyne honeycomb dystrophy (Stone et al. 1999; Guymer et al. 2002), respectively, were targeted for analysis.

To determine whether or not the previously described mutation in codon 5345 of the hemicentin-1 gene, resulting in conversion of a glutamine to an arginine, was present among family members, primers were designed to amplify exon 104 (forward primer 5′-tttcttttttatatcat-ggc-3′; reverse primer 5′-cacatactttgatcagtaag-3′). Standard conditions were used for PCR amplification, followed by purification of the product with an ExoSAP-IT (USB Corporation) treatment to remove the residual primers. The purified amplicons were subjected to au-

tomated sequencing with the BigDye terminator kit, using the forward primer, and were run on the ABI 3700 to identify the mutation.

Individuals with ARMD scores >12, clinically considered equivalent to the end stages of ARMD with geographic atrophy or neovascular disease, were selected from three families that were linked to chromosome 2. Primers spanning each of the 11 exons in EFEMP1 were used to amplify the DNA from these individuals, using previously described conditions (Stone et al. 1999). The resulting products were purified with ExoSAP-IT (USB Corporation) and were subjected to automated sequencing to identify mutations in EFEMP1.

We also genotyped four SNPs in the hemicentin-1 gene and two SNPs in the EFEMP1 gene. A Taqman assay (Assays on Demand, Applied Biosystems) was used to interrogate each SNP in a final volume of 25μl using manufacturer's protocols. The following SNPs were genotyped: in hemicentin-1, rs1475113 in intron 4, rs743137 in intron 36, hCV625089 in intron 86, and rs680638 in intron 105; and, in EFEMP1, rs1430193 in intron 4 and rs2277887 in intron 2.

Statistical Methods

Error checking and relationship testing.—Inconsistencies in the segregation of the genotypes within families were examined using MARKERINFO (S.A.G.E. v4.4). Individuals who demonstrated Mendelian inconsistencies at multiple markers that could not be resolved by retyping were treated as missing for the purpose of this analysis. In total, 0.24% of the data were treated as missing. We also checked the marker data for any significant departures from Hardy-Weinberg proportions. We then established the allele frequencies for each genetic marker by simple gene counting (disregarding relationships). Critical results were also verified by comparing them with the maximum likelihood estimates of the allele frequencies obtained using the S.A.G.E. program FREQ.

Prior to performing the linkage analysis, we reclassified the sib pairs in each pedigree according to their likely true relationship, utilizing the S.A.G.E. program RELTEST. RELTEST classifies relationships by using a Markov process model of allele sharing along the chromosomes (Olson 1999). The probability of misclassification depends on the total length of the genome scan and overall marker informativeness. It is possible for individual pairs to be misclassified if one or both members have a high proportion of missing genotypes. We reclassified four individuals in three full sibships as halfsibs, and three individuals in three full sibships as unrelated, and hence their data were deleted. There was only one reclassification in which one member of a sibpair had as much as 10% missing data.

Linkage analyses.—The power of a model-free quantitative trait linkage analysis depends on the scale of measurement (Wilson et al. 1991). In order to perform a Box-Cox power transformation of the data (Box and Cox 1964), all the measurements must be positive. For this reason, we adjusted the scores to age 80, as did Heiba et al. (1994), by adding $13.62391 - 0.51210 \times 80 - 0.00581 \times 80^2$ to the residuals obtained from the regression analysis on age and age^2. This resulted in 18 of the age-adjusted scores being >15, the highest score in the revised ARM scoring system. Therefore, these 18 age-adjusted scores were winsorized, replacing them with the 19th-largest score. One age-adjusted score was negative and was replaced with zero.

A commingling analysis was performed to compare the distribution of the age-adjusted scores for the FARMS data with that of Beaver Dam data (Heiba et al. 1994), using the program SEGREG in S.A.G.E.. It was found that a two-mean model similar to that for the Beaver Dam data fitted the best; the estimate of the power transformation was 0.80, similar to that (0.76) for the Beaver Dam data. Therefore, the age-adjusted scores were raised to the power of 0.80 prior to linkage analysis.

Genotypes from all family members were used to calculate multipoint identity by descent (IBD) allele sharing distributions using the GENIBD program of S.A.G.E.. SIBPAL, a model-free S.A.G.E. linkage program was then used in our study to perform the linkage analysis using all possible sib pairs. Evidence for linkage was evaluated by a Haseman-Elston regression (Haseman and Elston 1972; Elston et al. 2000) as implemented in SIBPAL, using the newest adaptation of the method, which transforms the sib pair's trait values to a weighted combination of the squared trait difference and squared mean corrected trait sum, allowing for the nonindependence of sib pairs (W4 option) (Shete et al. 2003). Apart from relative ease of analysis, an advantage of restricting the analysis to full-sibling relationships (other than to calculate the allele sharing by pairs of sibs) is the ease with which valid P values can then be obtained by a permutation test that fully allows for the correlational structure of the data. Thus, all multipoint results that were nominally significant were verified by comparison to the null permutation distribution, using a sample of up to 100,000 replicate permutations of the allele sharing data, the permutation being both within sibships and across sibships of the same size, as implemented in SIBPAL. Multipoint empirical P values are reported in the results for specific marker locations. We should note that these empirical P values are not corrected for multiple testing but can be interpreted as genomewide significance levels following the locus-counting method of Wiltshire et al. (2002). Linkage analyses were performed for all 34 families jointly, followed by

independent analysis of each of the 18 largest families to identify families linked to specific chromosomal locations. Of these families, 13 were included in the tests for heterogeneity, but all 34 families were used to test for epistasis.

Analyses to identify heterogeneity and epistasis.—To formally confirm findings of linkage heterogeneity, tests of statistical interaction were conducted between a family effect and allele sharing in regions showing evidence for linkage in the 13 families containing at least 5 sib pairs (the number of sib pairs in a family ranges up to 76). The test of statistical interaction was done by fitting (1) a reduced regression model that included the main effect of allele sharing at a location, along with an intercept and 12 family effects, and (2) a full regression model that also included the 12-family effect by allele-sharing interaction terms. Equivalently, the reduced model includes a separate intercept for each family (as 13 nuisance parameters), together with a single common regression on allele sharing (a total of 14 parameters), whereas the full model includes these same 13 intercepts and regression on allele sharing for each of the 13 families (26 parameters), thus allowing for linkage heterogeneity. Denoting the residual sum of squares SSE_R and SSE_C for the reduced and full models, respectively, and MSE_C for the mean square error for the full model, the test statistic $(SSE_R - SSE_C)/(12 \times MSE_C)$ has an F-distribution with numerator and denominator df 12 and $n - 26$, respectively, where n is the number of sib pairs, if the sib pairs are independent. Because the sib pairs are not independent, we take the denominator df to be the effective number of independent sib pairs -26, where the effective number of independent sib pairs was taken to be the number of sibs minus the number of sibships (Wilson and Elston 1993). It should be noted that when a weighted average of the squared trait difference and the squared mean-corrected trait sum is used as the dependent variable in the Haseman-Elston regression (Shete et al. 2003), the weights depend on the model that is fitted, with the result that the dependent variable changes with the model. To avoid this difficulty, all heterogeneity tests were performed using the mean-corrected trait cross-product (Elston et al. 2000) as the dependent variable. For all seven regions where the overall P value was <.002 for linkage analysis, we initially tested for heterogeneity at the most significant location. Whenever the P value of the heterogeneity test was <.01, surrounding points were further tested for heterogeneity.

We tested for epistatic interaction between locations on two different chromosomes using a new Haseman-Elston regression analysis model that included the product of the estimated proportions of alleles shared at each location. We did this using a full model that included the interaction term in addition to an intercept and the two main effects—that is, the estimated proportions of

alleles shared at each location. To demonstrate that a negative result for such a test should not be interpreted as an indication that epistasis is not present, we also compared the full model with a model that included only an intercept and the interaction term.

Analysis of hemicentin-1 and EFEMP1 SNPs.—To eliminate a gene as a candidate gene for ARMD, a linkage analysis was carried out incorporating the SNPs within the gene as covariates in the new Haseman-Elston regression analysis. The purpose of this was to see whether the significance of linkage to ARMD was removed by adding the covariates into the regression model (Fulker et al. 1999). A full covariate model was initially constructed that included 6 covariates for each SNP: the mean-corrected sum, the difference and the mean-corrected cross-product of each of the dummy variables that coded the dominant and additive effects of the SNPs in the gene. Covariates resulting in unstable estimates because of extreme colinearity were eliminated from the regression equation. The final model included all the additive terms but no dominance terms, which destabilized the models.

For multiple SNPs in a candidate gene that accounted for all the linkage evidence, we used two ways to determine the haplotype of length n associated with high values of the trait ($n = 1,2,3,4$) from the results that yielded the largest P value indicated for each value of n. First, we looked at the sign of the coefficient of the additive effect sum in the Haseman Elston regression analysis; a positive sign would indicate association with the allele coded 2 in homozygotes and a negative sign would indicate association with the allele coded 0 in homozygotes (all heterozygotes were coded 1). Second, characterizing each allele by its additive effect, so that there are two effects associated with each SNP, we examined the 2^n possible haplotype effects for n SNPs and chose the haplotype with the largest effect.

Results

The data set for FARMS comprise 34 extended pedigrees with a total of 297 individuals and 349 sib pairs. The average number of individuals per pedigree $\pm$ SD was 12.18 ± 7.57, with a minimum of 4 and a maximum

Table 1

Descriptive Statistics for Probands and Other Relatives in the 34 Families with ARMD

Family Members	N	% Male	Average Age at Diagnosis [SD] (years)	Average ARMD Score [SD] (years)
Probands	34	23.5	78.7 [5.33]	13.10 [1.65]
Sibs of proband	85	38.8	73.7 [8.66]	7.69 [4.39]
Others	178	47.2	54.4 [11.63]	2.93 [2.09]
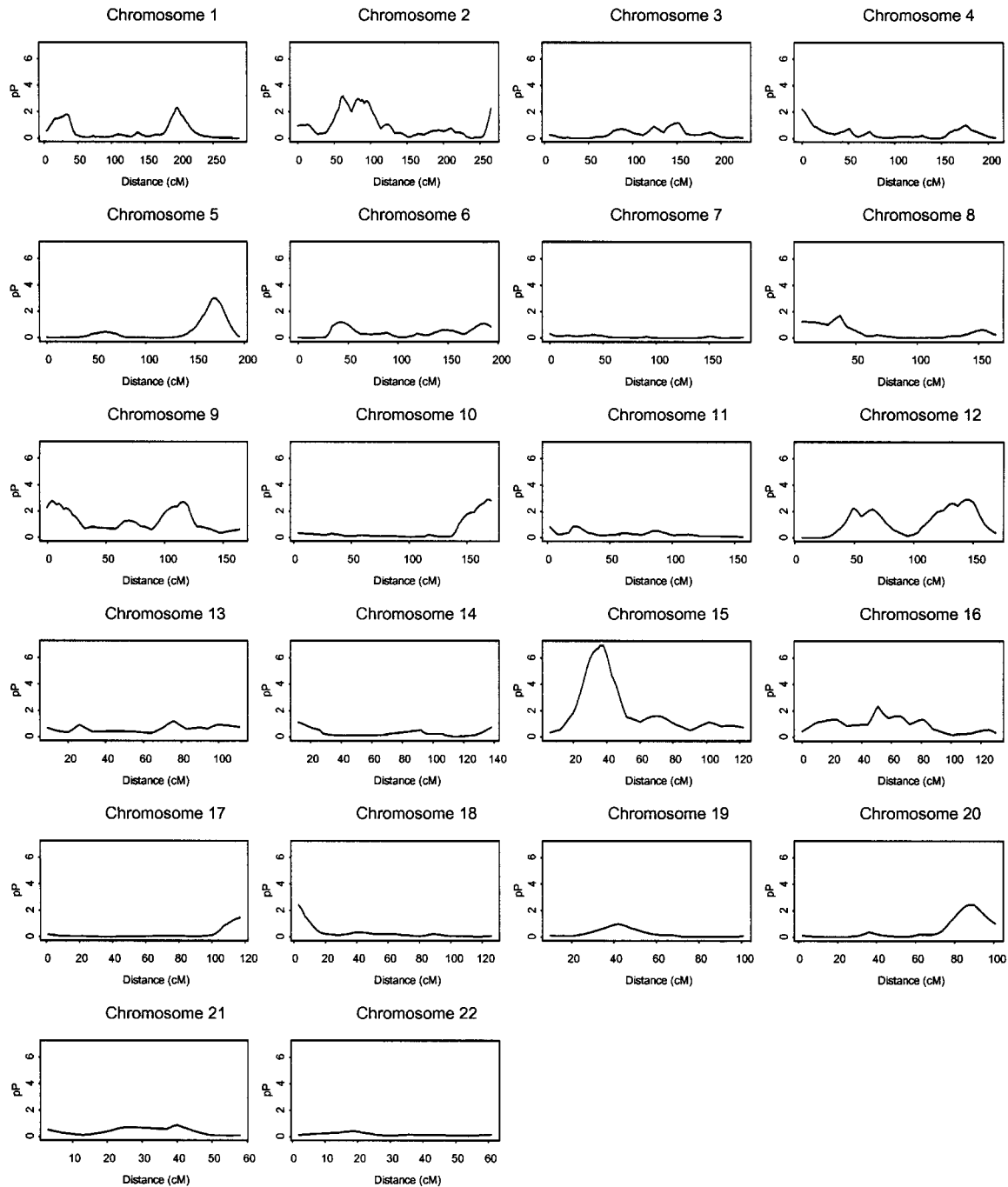
Figure 1 Multipoint results of the genomewide linkage scan for ARMD, using the Weber Panel 10 map spacing on 22 autosomes. For each chromosome, genetic distance (cM) is plotted on the X-axis against $pP = -\log_{10} (P \text{ value})$ on the Y-axis.

of 46 individuals. There were 100 sibships with an average size of 2.80 ± 1.77, with a minimum of 1 and a maximum of 9 individuals. As described earlier, families were ascertained through probands who had late-stage disease. The average ARMD score $\pm$ SD for the probands was 13.1 ± 1.65 (table 1). Of the 34 families,

22 had at least one other sib with a score >12 in at least one eye.

Genome Scan

The results of the full genome scan are presented in figure 1. We observed 13 regions on 11 chromo-

Table 2

Genetic Locations and Multipoint *P* Values for Markers and Interpolated Locations Showing Possible Linkage ($P \leq .01$) on Chromosomes 1, 2, 4, 5, 9, 10, 12, 15, 16, 18, and 20 for ARMD

Chromosome and Location (cM)	Marker	*P* Value
Chromosome 1:		
194		.0077
196		.0052
198		.0054
200		.0083
Chromosome 2:		
54		.0096
56	D2S1788	.0065
58		.0019
60		7.8×10^{-4}
62		6.7×10^{-4}
64	D2S1356	.0011
66		.0015
68		.0023
70		.0039
72		.0066
76		.0050
78		.0024
80		.0014
82		.0011
84		.0011
86		.0014
87	D2S441	.0016
88		.0013
90		.0016
91	D2S1394	.0023
92		.0020
94		.0016
96		.0016
98		.0023
100		.0041
102		.0085
264		.0094
265	D2S2986	.0054
Chromosome 4:		
0	D4S3360	.0065
2		.0084
Chromosome 5:		
162		.0078
164		.0037
166		.0018
168		.0011
170		.0010
172		.0012
174		.0017
175	D5S1456	.0021
176		.0026
178		.0049
Chromosome 9:		
0	D9S1779	.0057
2		.0026
4		.0018
6		.0020
8	D9S1871	.0032
10		.0028
12		.0036
14		.0069

(continued)

Table 2 (continued)

Chromosome and Location (cM)	Marker	*P* Value
Chromosome 9 (continued):		
16		.0060
18		.0069
102		.0090
104	D9S910	.0066
106		.0052
108		.0045
110		.0044
111	D9S938	.0045
112		.0033
114		.0022
116		.0019
118		.0024
120	D9S930	.0038
Chromosome 10:		
158		.0072
160		.0045
162		.0031
164		.0024
165	D10S1248	.0022
166		.0017
168		.0012
170		.0013
171	D10S212	.0015
Chromosome 12:		
48		.0080
49	D12S1042	.0056
50		.0059
52		.0079
62		.0088
64		.0071
65	D12S297	.0066
66		.0072
68		.0092
122		.0089
124		.0082
125	D12S2070	.0082
126		.0065
128		.0042
130		.0029
132		.0025
134		.0026
136		.0033
137	D12S395	.0039
138		.0031
140		.0021
142		.0015
144		.0012
146		.0012
148		.0014
150	D12S2078	.0019
152		.0037
154		.0085
Chromosome 15:		
22		.0037
24		5.9×10^{-4}
26		6.8×10^{-5}
28		7.8×10^{-6}
30		1.3×10^{-6}

(continued)

Table 2 (continued)

Chromosome and Location (cM)	Marker	P Value
Chromosome 15 (continued):		
32		3.9×10^{-7}
34		2.2×10^{-7}
35	GATA50C03	2.0×10^{-7}
36		1.2×10^{-7}
38		1.2×10^{-7}
40		5.6×10^{-7}
42		6.3×10^{-6}
43	D15S659	2.2×10^{-5}
44		3.7×10^{-5}
46		1.6×10^{-4}
48		.0011
50		.0068
Chromosome 16:		
50		.0070
51	D16S769	.0046
52		.0064
Chromosome 18:		
3	GATA178F11	.0038
5		.0079
Chromosome 20:		
84		.0069
86		.0041
88		.0034
90	D20S451	.0035
92		.0063

NOTE.—Distances are in Kosambi cM from the most telomeric p-arm marker.

somes (chromosomes 1q31, 2p21, 4p16, 5q34, 9p24, 9q31, 10q26, 12q13, 12q23, 15q21, 16p12, 18p11, and 20q13) with a nominal multipoint significance level of $P \leqslant .01$, or LOD $\geqslant 1.18$ (table 2). Our strongest evidence of linkage was observed on chromosome 15q with markers GATA50C03 and D15S659; marker GATA50C03 exhibited a multipoint P value of 1.98×10^{-7} (empirical $P \leqslant 1.0 \times 10^{-5}$; single-point $P = 3.6 \times 10^{-7}$) meeting criteria for highly significant linkage (Lander and Kruglyak 1995). This region on chromosome 15q is novel. A weak linkage signal on chromosome 15q was observed in our previous genome scan (Schick et al. 2003). The remainder of the regions demonstrated moderate evidence for linkage with multipoint P values ranging from .00016 to .0068. One possible region of interest was located on chromosome 1q31, with the greatest significance at 196 cM (multipoint $P = .0052$; empirical $P \leqslant .0149$; single-point $P = .0117$). Our results confirm previous reports of this linkage on 1q31 (Klein et al. 1998a). Five markers on chromosome 2 demonstrated evidence of linkage, with marker D2S1356 having the greatest significance (multipoint $P = .0024$; empirical $P \leqslant .0041$; single-point $P = 2.6 \times 10^{-4}$). This region on chromosome 2 has previously been implicated in Doyne honeycomb dystrophy, for which mutations in the EFEMP1 gene have been

discovered (Stone et al. 1999). We found suggestive evidence of linkage on four other chromosomes 4, 5, 9, and 10, at markers D4S3360 (multipoint $P = .0065$; empirical $P \leqslant .0087$; single-point $P = .0031$), D5S1456 (multipoint $P = .0021$; empirical $P \leqslant .0049$; single-point $P = .0058$), D9S1871 (multipoint $P = .0032$; empirical $P \leqslant .0048$; single-point $P = .0079$), D9S938 (multipoint $P = .0051$; empirical $P \leqslant .008$; single-point $P = .0017$), D10S1248 (multipoint $P = .0022$; empirical $P \leqslant .0037$; single-point $P = .0971$), respectively. Linkage to 10q26 initially reported by Weeks et al. (2001) for a binary ARMD trait, was recently confirmed by Majewski et al. (2003), and now has been validated in a quantitative trait linkage analysis for ARMD. However, the location of the linkage signals on chromosomes 5q34 and 9p24 are not identical to those reported elsewhere (Weeks et al. 2001; Majewski et al. 2003). The location of the second signal on chromosome 9 at marker D9S938 is within 15–20 cM of the peak location of the report of linkage at 9q33 by Majewski et al. (2003) and represents a possible confirmation of this linkage signal. Five markers in two possible regions of linkage were also found on chromosome 12q13 and 12q23, with marker D12S2078 presenting the highest significance (multipoint $P = .0019$; empirical $P \leqslant .002$; single-point $P = .0038$). Marker D12S2078 is within 18 cM of markers D12S1300 and PAH, which showed evidence of linkage in our previous community-based sample (Schick et al. 2003). Finally, chromosomes 16, 18, and 20 also showed linkage evidence at markers D16S769 ($P = .0050$; empirical $P \leqslant .0121$; single-point $P = .0140$), GATA178F11 ($P = .0047$; empirical $P \leqslant .0033$; single-point $P = .0014$), and D20S451 ($P = .0034$; empirical $P \leqslant .0052$; single-point $P = .0061$), respectively. The last three loci are novel and are being reported here for the first time.

Chromosome 15 Fine Mapping

Fine mapping was conducted on chromosome 15 using 14 new markers spanning the initial region. The result, presented in figure 2, shows a clear confirmation of the already overwhelmingly significant evidence of linkage. Significant linkage evidence ($P < 1.0 \times 10^{-5}$) extends over a 10-cM area on chromosome 15 containing four markers (table 3). The peak marker in this region is marker D15S1012 ($P = 3.5 \times 10^{-7}$). Our results are consistent with a major locus for ARMD susceptibility on 15q.

Chromosome 12 Fine Mapping

We decided to fine-map the area of significance on chromosome 12 indicated by our genome scan because there was an overlap between this region and the result discovered in the Beaver Dam ARMD genome scan
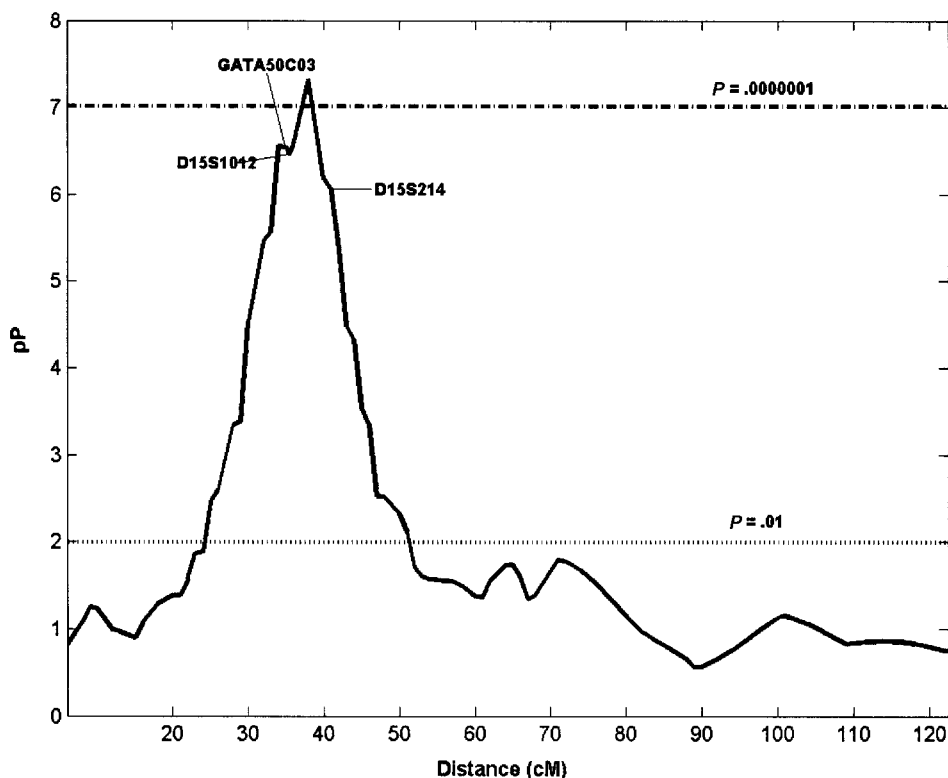
Figure 2   Fine-mapping multipoint results on chromosome 15q for ARMD. Genetic distance (cM) is plotted on the *X*-axis against $pP = -\log_{10}$ (*P* value) on the *Y*-axis. Horizontal lines are drawn at $P = .0001$ and $P = .000001$.

(Schick et al. 2003). Thus, 25 additional markers on chromosome 12 were added to the study using the genetic distances provided at the Web site of the Marshfield Center for Medical Genetics. On comparing the initial genome scan results with the fine map and the previous data from the BDES study, we observed a shift in the linkage signal to a slightly more distal location. Figure 3 shows a region of 36.4 cM with five markers presenting a significant link with ARMD at $P < .01$. The peak marker is D12S2078 ($P = .0016$) (table 3). However, markers D12S1300 and PAH, which were significant in the previous study (Schick et al. 2003), did not show any evidence of significant linkage, and it is possible that several ARMD loci reside on chromosome 12q.

Chromosome 1 Fine Mapping

A candidate gene for the exudative autosomal dominant form of ARMD has been reported to be located within a 9-cM region on chromosome 1q25-q31 between the markers D1S466 and D1S413 (Klein et al. 1998*a*). Because we obtained evidence of linkage with marker D1S518, we also fine mapped a 12-cM region that included markers D1S466, D1S518, D1S202, D1S2625, D1S413, and D1S1660 (fig. 4 and table 3). The linkage evidence ($P \le .01$) extends over a 6.2-cM

area containing three markers (table 3), with marker D1S202 on 1q31 showing the greatest significance ($P = .0014$). Our results confirm previous reports of linkage on 1q31 (Klein et al. 1998*a*). In summary, our linkage analysis of ARMD provides strong evidence that markers located on chromosomes 15, 12, and 1 demonstrate linkage.

Family-by-Family Dissection of the Linkage Signals

To determine which families were linked to specific chromosomes, we analyzed the largest 18 of the 34 families individually. The results of these linkage analyses are presented in figure 5. We observed that most families contributed to the linkage signal on more than one chromosome (e.g., family 460), suggesting that, in these families, ARMD is an oligogenic disorder. Wiltshire et al. (2002) showed how locus counting on genome scan data can be used to determine that more regions demonstrate evidence of linkage across a range of LOD scores than would be expected by chance alone. For example, for a typical autosomal genome scan with average marker density of 10 cMs (15% missing genotypes), an independent region of linkage with a LOD score of 1.51–1.55 is expected to occur once by chance alone. We observe that, in family 460, eight regions show *P* values

Table 3

Genetic Locations and Multipoint *P* Values for Fine-Mapping Markers and Interpolated Locations Showing Possible Linkage (*P* ≤ .01) on Chromosomes 1, 12, and 15 for ARMD

Chromosome and Location (cM)	Marker	*P* Value
Chromosome 1:		
200		.0079
201.6	D1S202	.0013
202		.0013
202.2	D1S518	.0020
204		.0016
206		.0050
206.2	D1S2625	.0070
Chromosome 12:		
46		.0088
47	D12S1042	.0054
48		.0049
50		.0037
52		.0030
54		.0027
56		.0028
58		.0033
60		.0042
62		.0055
63	D12S297	.0056
64		.0066
66		.0087
119.6	D12S1344	.0048
119.6	D12S1583	.0027
120		.0024
122		.0014
124		.0014
125.3	D12S2070	.0018
126		.0015
128		9.5×10^{-4}
130		6.9×10^{-4}
132		6.8×10^{-4}
134		9.1×10^{-4}
136		.0015
136.8	D12S395	.0019
138		.0016
140		.0012
142		9.8×10^{-4}
144		8.8×10^{-4}
146		9.1×10^{-4}
148		.0011
150		.0014
150	D12S2078	.0016
152		.0022
154		.0043
156		.0095
Chromosome 15:		
25.9	D15S1007	.0035
26		.0026
28		4.5×10^{-4}
28.4	D15S1040	4.2×10^{-4}
30		3.0×10^{-5}
32		3.5×10^{-6}
32.6	D15S118	2.7×10^{-6}
34		2.8×10^{-7}
34.8	GATA50C03	2.8×10^{-7}

(*continued*)

Table 3 (continued)

Chromosome and Location (cM)	Marker	*P* Value
Chromosome 15 (continued):		
36	D15S1012	3.5×10^{-7}
36		2.7×10^{-7}
38		5.0×10^{-8}
40		6.7×10^{-7}
40.3	D15S214	9.0×10^{-7}
42		4.2×10^{-6}
43.5	D15S659	3.3×10^{-5}
44		4.7×10^{-5}
45.6	D15S143	2.8×10^{-4}
46		4.4×10^{-4}
47.9	D15S209	.0030
48		.0030
50		.0047
51.2	D15S117	.0076

NOTE.—Distances are in Kosambi cM from the most telomeric p-arm marker.

≤.0001, which supports the hypothesis of multigenic inheritance.

Numerous families jointly contributed to linkage signals on chromosomes 9p, 12q, and 15q. In contrast, only two families contributed very strongly to the linkage signal on chromosome 10q26. Moreover, even on a single chromosome, there is sizeable variance in the location of the family-specific linkage signal (Cordell 2001). For example, over the region of 35–43 cM on chromosome 15 that contains the location that shows the strongest genomewide linkage evidence (36 cM; $P = 3.5 \times 10^{-7}$), the results demonstrate that only family 446, 460, and 465 individually present evidence of linkage at the $P < .01$ level of significance. Other families do contribute to the linkage evidence, but the signal is weaker and occasionally shifted, as seen in family 440. We observe that the evidence from individual families suggests that additional loci, not reaching statistical significance when the data are analyzed as an aggregate, may play a role in the pathogenesis of ARMD—for example, the loci on chromosomes 7p, 13p, and 17q. Multiple weaker signals are observed on practically every chromosome, which may simply be type 1 error or may be the product of genetic modifiers of weak effect.

Heterogeneity Analysis

The presence of linkage heterogeneity among families was tested at the following seven locations in the genome: 5q34, 9p24, 9q31, 10q26, 12q13, 12q23, and 15q21. The *P* values of the heterogeneity tests performed at the initial locations of all seven regions are <.01. Furthermore, these heterogeneity tests resulted in significance at the 0.001 level in the five regions ranging from 164 to 175 cM on chromosome 5, from 0 to 10 cM and
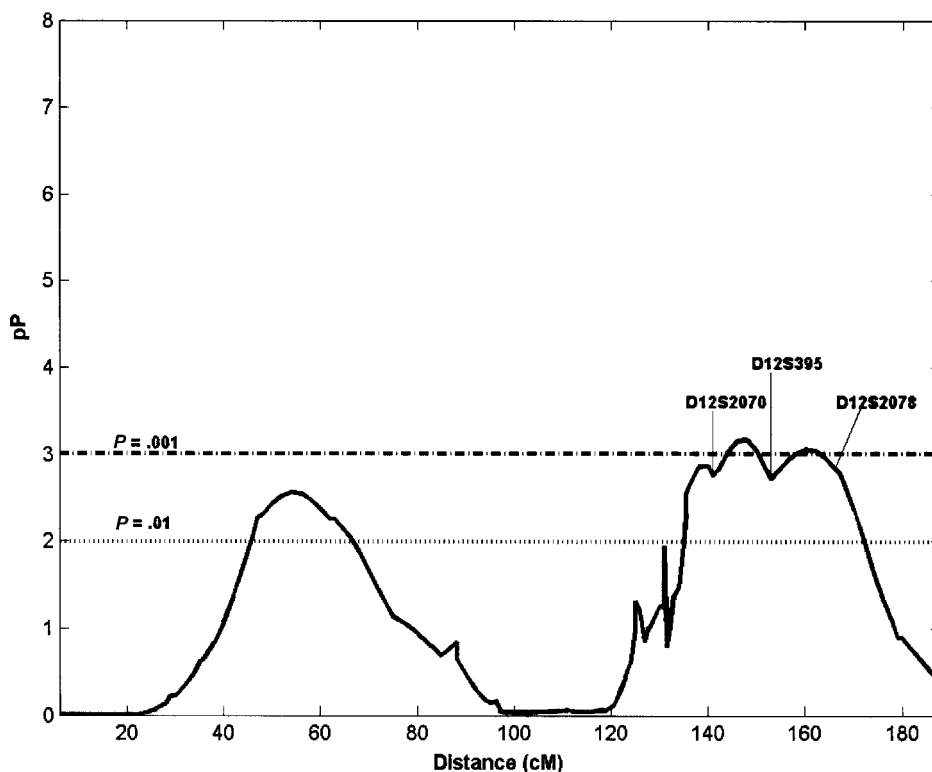
Figure 3   Fine-mapping multipoint results on chromosome 12q for ARMD. Genetic distance (cM) is plotted on the *X*-axis against $pP = -\log_{10}$ (*P* value) on the *Y*-axis. Horizontal lines are drawn at *P* = .01 and *P* = .001.

from 111 to 122 cM on chromosome 9, from 164 to 171 cM on chromosome 10 and from 30 to 43 cM on chromosome 15. This analysis confirmed that there is significant linkage heterogeneity among the pedigrees in these regions (table 4). On the other hand, over the regions from 56 to 68 cM on chromosome 2 and from 138 to 150 cM on chromosome 12, the *P* values for the heterogeneity tests at some locations are >.01. This result does not strongly support the hypothesis of heterogeneity in these regions, contrary to the trends evident in the pedigree-by-pedigree linkage analysis (table 5 and fig. 5).

Epistasis Analysis

The most significant locations in the regions with nominal linkage evidence of ⩽*P* = .002 are—apart from 36 cM on chromosome 15—62 cM on chromosome 2, 170 cM on chromosome 5, 4 cM and 116 cM on chromosome 9, 164 cM on chromosome 10, and 138 cM on chromosome 12. Each of these six locations was tested in turn for epistatic interaction with the chromosome 15 location. When the full regression model is used, although no significant interactions are observed, the significance of each individual locus is much reduced, to the extent that *P* > .05 for the locations on chro-

mosomes 9, 10, and 12. However, if no main effects are fitted in the model, then the extremely small *P* values for each one of the interaction terms (table 6) would indicate that we cannot exclude genetic interaction between the location of 36 cM on chromosome 15 with each of the locations listed above. These results indicate extreme confounding and demonstrate that it is difficult to find evidence for epistasis and that models of heterogeneity and epistasis may be irrevocably confounded in this type of analysis.

Mutation Analysis of Candidate Genes

Sequencing exon 104 of hemicentin-1 in "affected" individuals (i.e., those with ARMD scores >12) from families linked to chromosome 1q31 (*N* = 3) did not demonstrate any evidence of mutations in this exon. We also sequenced all 11 exons of EFEMP1 in "affected" family members from families linked to chromosome 2p16 (*N* = 3). No mutations were observed. To eliminate hemicentin-1 and EFEMP1 as the putative susceptibility genes, we also genotyped SNPs in these genes and analyzed these SNPs as covariates in a linkage analysis. This analysis was performed in a subsample containing the pedigrees linked to 1q31 and 2p16. Thus,
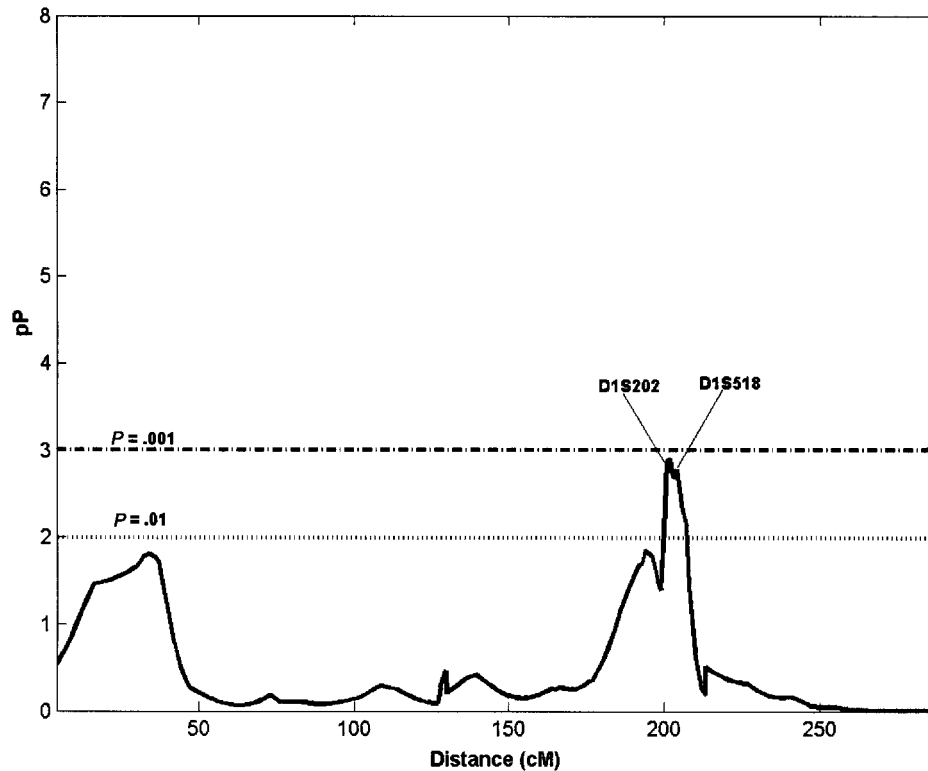
Figure 4   Fine-mapping multipoint results on chromosome 1q for ARMD. Genetic distance (cM) is plotted on the X-axis against $pP = -\log_{10}$ (P value) on the Y-axis. Horizontal lines are drawn at $P = .01$ and $P = .001$.

145 and 189 sib pairs were genotyped and analyzed for hemicentin-1 and EFEMP1, respectively.

SNP Analysis

The following four SNPs within the hemicentin-1 gene on chromosome 1q31 were analyzed: rs1475113 (H1), rs743137 (H2), hCV625089 (H3), and rs680638 (H4). First, standard linkage models without covariates—but including the SNPs as outcome variables, to estimate allele sharing at all locations—were constructed. Then, as described in the "Methods" section, we simultaneously modeled all four SNPs in the Haseman-Elston regression analysis as covariates (predictors), to determine if the SNPs were able to account for all the variance at 1q31 and to explain the linkage results. We observed that inclusion of the covariates associated with the dominant effects led to numerical instability, because the SNPs were located within the same gene and there is significant colinearity involved when all 24 covariate terms for the SNPs are included in the same model. Thus, the dominance terms were excluded from the analyses, leaving a total of 12 covariates in the full regression equation.

Inclusion of the SNPs as markers in the linkage model led to a significant increase in the overall evidence for linkage at 1q31 (table 7). For example, at the location of the SNP rs680638 (196.56 cM), the P value for linkage obtained from a multipoint analysis that included the SNPs as markers but did not include covariates is 7.2×10^{-5}. We compared this model to those where SNPs were sequentially dropped out of the analysis as covariates (table 8). We observed a significant decline in the level of significance when all 12 additive-effect covariates were included in the regression ($P = .51$), suggesting that inclusion of all four SNPs accounted for virtually all the linkage evidence. Interestingly, the additive-effect covariate terms from at least two SNPs was necessary for the linkage P value to be >.05. Among all the combinations of the covariates corresponding to three SNPs, the combination with SNPs rs1475113 (H1), rs743137 (H2), and rs680638 (H4) has the largest P value ($P = .44$), suggesting that these three SNPs account for the majority of the linkage. Among the two SNP combinations, rs1475113 (H1) and rs680638 (H4) shows the largest P value ($P = .23$). We also examined the haplotypic combinations that best accounted for the significant results. Except for haplotypes of length 2, the two methods described in the "Methods" section resulted in the same susceptibility-associated haplotypes, which can be seen, in table 8, to be consistent with each

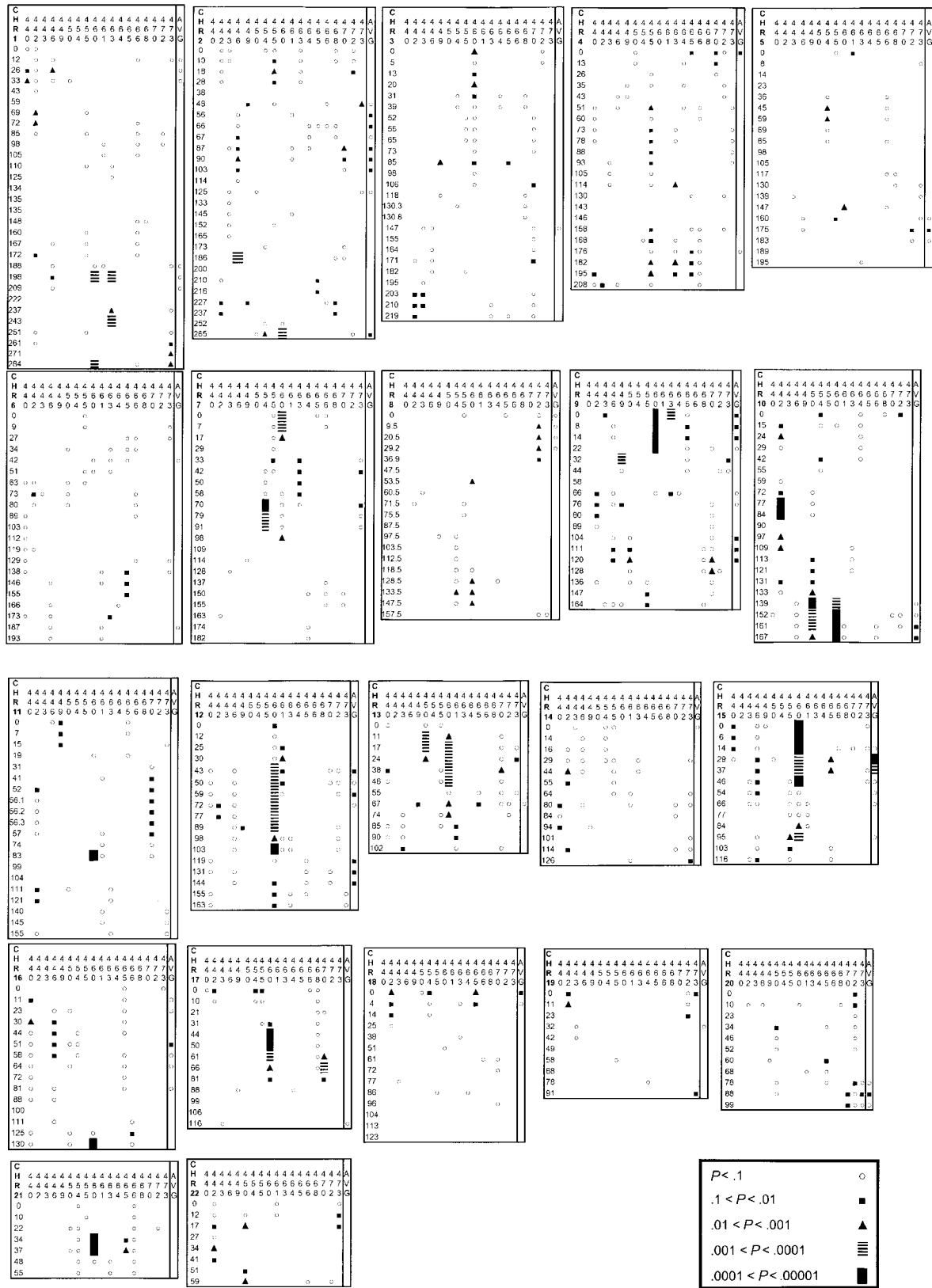**Figure 5** Family-by-family multipoint results of the genomewide linkage scan for ARMD, using the Weber Panel 10 map spacing on 22 autosomes. Symbols corresponding to $pP = -\log_{10}$ (P value) are presented for each of 18 families (family number on X-axis). For each chromosome, genetic distance (cM) is plotted on the Y-axis. Each box corresponds to a chromosome, with the chromosome number given in the top left-hand corner.

Table 4

Results of the Heterogeneity Analysis on Chromosomes 5, 9, 10, and 15, Demonstrating That Significant Familial Variability Exists for ARMD

Chromosome and Location (cM)	Marker	Linkage	F Test
Chromosome 5:			
164		.0037	4×10^{-4}
166		.0018	5×10^{-4}
168		.0011	8.0×10^{-4}
170		.0010	.0012
172		.0012	.0018
174		.0017	.0027
175	D5S1456	.0021	.0034
Chromosome 9:			
0	D9S1779	.0057	$<1 \times 10^{-5}$
2		.0026	$<1 \times 10^{-5}$
4		.0018	$<1 \times 10^{-5}$
6		.0020	$<1 \times 10^{-5}$
8	D9S1871	.0032	$<1 \times 10^{-5}$
10		.0028	$<1 \times 10^{-5}$
111	D9S938	.0045	1×10^{-4}
112		.0033	1×10^{-4}
114		.0022	1×10^{-4}
116		.0019	2×10^{-4}
118		.0024	.0017
120	D9S930	.0038	$<1 \times 10^{-5}$
122		.0121	.0873
Chromosome 10:			
164		.0024	2×10^{-4}
165	D10S1248	.0022	3×10^{-4}
166		.0017	3×10^{-4}
168		.0012	4×10^{-4}
170		.0013	4×10^{-4}
171	D10S212	.0015	8×10^{-4}
Chromosome 15:			
32		3.9×10^{-7}	$<1 \times 10^{-5}$
34		2.2×10^{-7}	$<1 \times 10^{-5}$
35	GATA50C03	2.0×10^{-7}	$<1 \times 10^{-5}$
36		1.2×10^{-7}	$<1 \times 10^{-5}$
38		1.2×10^{-7}	$<1 \times 10^{-5}$
40		5.6×10^{-7}	$<1 \times 10^{-5}$
42		6.3×10^{-6}	$<1 \times 10^{-5}$

NOTE.—The P values associated with the overall linkage test, as well as these associated with the heterogeneity F statistic, are shown.

other. The haplotypes of length 2 associated with the P value .2275 were different, and neither was consistent with the haplotypes of length 1, 3, and 4. This leads us to conclude that at least two SNPs, rs1475113 (H1) and rs680638 (H4), and the corresponding haplotypes are tightly associated with a causative variant (table 8). Thus, the hemicentin-1 gene cannot be eliminated as a candidate gene for ARMD. Interestingly, SNP rs680638 is located in intron 105, in close proximity to the original reported mutation in exon 104 (Schultz et al. 2003). Our sequencing analysis of the linked families excluded

exon 104; however, mutations in other nearby exons cannot be eliminated as yet.

Two SNPs within the EFEMP1 gene, rs1430193 (E1) and rs2277887 (E2), were targeted for analysis as covariates in a Haseman-Elston regression. The dominance terms for both SNPs and the additive effects corresponding to rs2277887 provided unstable estimates, and were not included as covariates in the regression equation. The most significant location for linkage on chromosome 2, after inclusion of the SNPs as markers (outcome variable), but not as covariates, was at 89 cM on chromosome 2 ($P = 7.3 \times 10^{-5}$) (table 9). There was no major difference in the P value for models with and without the three additive-effect covariates corresponding to rs1430193 (E1) ($P = 7.3 \times 10^{-5}$ without SNPs and $P = 7.0 \times 10^{-5}$ with additive effect of SNP E1). Thus, addition of covariates (SNPs) did not take away any linkage evidence at the most significant location on chromosome 2, indicating that the EFEMP1 gene is neither partially causative nor tightly associated with a causative gene. To further confirm this result, the linkage signals on chromosome 2 obtained using multipoint analyses were compared with and without the two SNPs. When the SNPs were included in the analysis, the linkage evidence generally become weaker (80 cM, $P = .0023$) near the EFEMP1 locus, as opposed to the linkage signal without the SNPs (80 cM, $P = 6.6 \times 10^{-5}$). This supports our previous result that the EFEMP1 gene can be eliminated as a candidate gene for ARMD.

Table 5

Results of the Heterogeneity Analysis on Chromosomes 2 and 12, Demonstrating That Little Significant Familial Variability Exists for ARMD at These Loci

Chromosome and Location (cM)	Marker	Linkage	F Test
Chromosome 2:			
56	D2S1788	.0065	.2191
58		.0019	.1021
60		7.8×10^{-4}	.0300
62		6.7×10^{-4}	.0057
64	D2S1356	.0011	9×10^{-4}
66		.0015	.0053
68		.0023	.0286
Chromosome 12:			
138		.0031	.0109
140		.0021	.0061
142		.0015	.0043
144		.0012	.0051
146		.0012	.0097
148		.0014	.0184
150	D12S2078	.0019	.0264

NOTE.—The P values associated with the overall linkage test, as well as these associated with the heterogeneity F statistic are shown.

Table 6

Comparison of Allele Sharing (π-hat) in Models With and Without Epistasis Testing of Main Effects and Interaction Models for Epistasis

			P Value for Model					
			Main Effects		Main Effects + Interaction			Interaction
Chromosome	Location (cM)	π-i[a] Alone	π-i	π-15	π-i	π-15	Interaction	Alone
2	62	6.7×10^{-4}	5.9×10^{-4}	1.1×10^{-7}	.0493	.0018	.5406	5.5×10^{-8}
5	170	9.7×10^{-4}	.0041	4.7×10^{-7}	.0462	.0052	.6667	9.6×10^{-8}
9	4	.0018	.0071	4.5×10^{-7}	.0097	1.6×10^{-4}	.9113	1.9×10^{-6}
9	116	.0019	.0059	3.5×10^{-7}	.3458	.0270	.1909	6.6×10^{-8}
10	164	.0012	.0025	2.4×10^{-7}	.0521	.0013	.6625	3.4×10^{-7}
12	138	.0012	.0040	3.8×10^{-7}	.1612	.0190	.3754	3.8×10^{-8}

[a] π-i = the average allele sharing at a locus other than chromosome 15, i = 2, 5, 9, 10, and 12.

Discussion

In this study, we have successfully mapped a novel major locus and oligogenic determinants for ARMD susceptibility, by use of sib-pair allele-sharing methods in extended families. We have identified novel loci on chromosomes 15q21, 5q34, 9p24, 12q13, 16p12, 18p11, and 20q13. Because of the availability of larger families, we were able to widen the scope of the allele-sharing methods to investigate 18 of the largest families individually. Examination of these results led us to conclude that ARMD pathogenesis is determined by locus heterogeneity and/or epistatic interaction between multiple susceptibility loci.

When we tested for evidence of heterogeneity at the seven loci that showed most evidence for linkage, we obtained significant support for this hypothesis at 5q34, 9p24, 9q31, 10q26, and 15q21. We investigated the epistatic interaction between the major locus on 15q21 and other minor loci on chromosomes 2p21, 5q34, 9p24, 9q31, 10q26, and 12q23. A full model for epistasis between two loci includes four epistatic components of variance (additive × additive, additive × dominant, dominant × additive, and dominant × dominant) (Tiwari and Elston 1997). However, to increase power, we included in our epistasis model only one of these four components, because there is a large degree of confounding among them. This is analogous to our including an additive genetic component, rather than both additive and dominant genetic components (which are also largely confounded) in our models without epistasis. Nevertheless, we initially found no significant evidence for epistasis. On the other hand, the significance of the individual locus variance components was greatly reduced in this analysis, and there was highly significant evidence for epistasis in a model that did not include any single-locus variance components, indicating confounding between the single- and two-locus components. Epistasis was also proposed by Majewski et al. (2003) in a recent model-based ARMD linkage scan in

70 families (344 affected and 217 unaffected). These investigators tested for epistatic interaction between markers at 3p13 and 10q26 and observed significant results. Although we did not test for interaction between markers at 3p13 and 10q26, our investigation on epistasis suggests that it may not be feasible to differentiate between models of epistasis and heterogeneity with this type of analysis. Thus far, very few moieties with an

Table 7

Summary of Linkage Analysis Results With and Without the Four SNPs in Hemicentin-1

Location (cM)	Marker	P Value	
		Without SNPs	With SNPs
20		.0099	.0111
21		.0097	.0107
22		.0095	.0103
23		.0095	.0101
24		.0096	.0099
25		.0097	.0098
26		.0099	.0098
27		.0102	.0098
28		.0106	.0100
194		.0058	.0026
195		.0029	9.4×10^{-4}
196		.0016	4.1×10^{-4}
197		9.7×10^{-4}	2.6×10^{-4}
198		7.2×10^{-4}	2.4×10^{-4}
199		6.6×10^{-4}	3.2×10^{-4}
200		7.2×10^{-4}	5.2×10^{-4}
200.32	rs1475113		6.2×10^{-4}
200.4	rs743137		6.0×10^{-4}
200.48	hCV625089		1.3×10^{-4}
200.56	rs680638		7.2×10^{-5}
201		9.1×10^{-4}	1.3×10^{-4}
202		.0012	7.0×10^{-4}
202.1	D1S518	.0014	.0016
203		.0016	.0017
204		.0019	.0021
205		.0024	.0026
206		.0032	.0036
207		.0047	.0052
208		.0072	.0079

Table 8

Modeling of Four SNPs in Hemicentin-1 as Covariates in the Haseman-Elston Regression

No. of SNPs and Model	P Value	Associated Haplotype[a]			
		H1	H2	H3	H4
0:					
Without Covariates	7.2×10^{-5}				
4:					
12 additive effects	.5147	G	A	T	T
3:					
Additive effects of H2H3H4	.1242				
Additive effects of H1H3H4	.2925				
Additive effects of H1H2H4	.4400	G	A		T
Additive effects of H1H2H3	.3755				
2:					
Additive effects of H1H2	.0368				
Additive effects of H1H3	.1436				
Additive effects of H1H4	.2275	A			T
Additive effects of H2H3	.0116				
Additive effects of H2H4	.0761				
Additive effects of H3H4	.0566				
1:					
Additive effects of H1	.0032				
Additive effects of H2	9.0×10^{-4}				
Additive effects of H3	.0181				
Additive effects of H4	.0446				T

NOTE.—Models ranging from inclusion of all SNPs (12 additive effects) to those with only a single SNP were tested.

[a] H1 = SNP rs1475113, H2 = SNP rs743137, H3 = SNP hCV625089, and H4 = SNP rs680638.

established role in ARMD are known that could drive the search for specific biological interactions, giving context to the epistatic (statistical) interactions identified in either our or other genome scans.

At the location of each linkage signal we canvassed the literature for genes known to play a role in ARMD and its clinical variants. Thus, in an effort to implicate specific candidate genes at 1q31 and 2p21, we tested SNPs at the hemicentin-1, and EFEMP1 genes, respectively. EFEMP1 is a member of the fibulin family (Timpl et al. 2003), a versatile group of extracellular matrix proteins. Mutations in EFEMP1 cause misfolding of the protein, followed by inefficient secretion of the mutant, which triggers accumulation of EFEMP1 in the RPE (Marmorstein et al. 2002). Although, EFEMP1 accumulates in the RPE, it is not a major component of drusen and the precise mechanism for drusen formation and culmination in advanced forms of Malattia Leventinese and Doyne honeycomb dystrophy (Stone et al. 1999; Guymer et al. 2002) is unknown. Both disorders are characterized by early-onset drusen formation with radial patterning of the drusen in the macula. Hemicentin-1 was identified as a positional candidate on 1q31 by Schultz et al. (2003) because of its similarity to EFEMP1, after 30 genes in the region were scanned.

Hemicentin-1 is a conserved extracellular member of the immunoglobulin superfamily (Vogel and Hedgecock 2001). Mutations in the him-4 locus, a *Caenorhabditis elegans* hemicentin ortholog, lead to tissue frailty and cell migration defects (Vogel and Hedgecock 2001).

Table 9

Summary of Linkage Analysis Results With and Without the Two SNPs in EFEMP1

Location (cM)	Marker	P Value	
		Without SNPs	With SNPs
56	D2S1788	.0073	.0076
57		.0046	.0049
58		.0030	.0032
59		.0020	.0022
60		.0014	.0016
61		.0011	.0013
62		9.4×10^{-4}	.0011
63		8.6×10^{-4}	9.9×10^{-4}
64	D2S1356	8.4×10^{-4}	9.7×10^{-4}
65		8.1×10^{-4}	9.6×10^{-4}
66		7.9×10^{-4}	9.6×10^{-4}
67		7.8×10^{-4}	9.8×10^{-4}
68		7.8×10^{-4}	.0010
69		7.9×10^{-4}	.0011
70		8.1×10^{-4}	.0012
71		8.6×10^{-4}	.0013
72		9.3×10^{-4}	.0015
73		.0010	.0018
74	D2S1352	.0011	.0021
75		6.6×10^{-4}	.0019
76		3.8×10^{-4}	.0018
77		2.3×10^{-4}	.0017
78		1.4×10^{-4}	.0018
79		9.1×10^{-5}	.0020
80		6.6×10^{-5}	.0023
80.61	rs1430193		.0025
80.62	rs2277887		.0025
81		5.3×10^{-5}	.0018
82		4.8×10^{-5}	8.2×10^{-4}
83		4.7×10^{-5}	3.9×10^{-4}
84		5.1×10^{-5}	2.1×10^{-4}
85		5.9×10^{-5}	1.4×10^{-4}
86		7.1×10^{-5}	1.1×10^{-4}
87	D2S441	8.8×10^{-5}	1.1×10^{-4}
88		6.0×10^{-5}	7.8×10^{-5}
89		5.4×10^{-5}	7.3×10^{-5}
90		7.1×10^{-5}	9.6×10^{-5}
91	D2S1394	1.3×10^{-4}	1.8×10^{-4}
92		1.2×10^{-4}	1.6×10^{-4}
93		1.3×10^{-4}	1.6×10^{-4}
94		1.4×10^{-4}	1.7×10^{-4}
95		1.7×10^{-4}	2.0×10^{-4}
96		2.3×10^{-4}	2.6×10^{-4}
97		3.4×10^{-4}	3.7×10^{-4}
98		5.6×10^{-4}	5.8×10^{-4}
99		9.5×10^{-4}	9.7×10^{-4}
100		.0017	.0017
101		.0029	.0028
102		.0049	.0048
103	D2S1790	.0079	.0077
104		.0101	.0098

Hemicentin-1 has been nominated as the ARMD1 locus, with mutations in exon 104 postulated to cause ARMD pathogenesis (Schultz et al. 2003).

Our SNP analysis suggests that variants in hemicentin-1, but not in EFEMP1, are tightly linked to an ARMD locus. We observed that the best-fitting model that accounted for a significant proportion of the linkage signal on 1q31 required a minimum of two SNPs. Of the four SNPs examined in hemicentin-1, SNPs rs1475113 (H1) and rs680638 (H4), located in introns 4 and 105, respectively, jointly explain the majority of the 1q31 linkage signal (table 8). When examining each SNP singly, we observed that rs680638 (H4) accounted for most of the linkage signal. The location of this SNP, between exons 104 and 105 in this large gene (transcript length 18,018 base pairs, 107 exons) is of considerable interest because of the initial report of mutations in exon 104 of hemicentin-1 causing ARMD1 (Schultz et al. 2003). Although we were unable to confirm the mutation in exon 104 via sequencing of affected individuals in the linked families, the ARMD susceptibility variant is likely to be in close proximity to this SNP. Our analysis indicates that a gene other than EFEMP1 at 2p21 is responsible for ARMD susceptibility. Because ARMD is oligogenic, with perhaps 8–10 predisposing loci, an exhaustive search at each linkage signal may involve analysis of innumerable candidate genes. We have presented an efficient strategy using SNPs as screening tools to limit the number of genes that would need to be scanned for specific mutations.

Comparison of our overall genome scan results with other published data reveals that we have novel results, but can also confirm several other linkage reports. Our group is the first to report the locus on chromosome 15q21. Of the other signals on chromosomes 1q31, 2p21, 4p16, 5q34, 9p24, 9q31, 10q26, 12q13, 12q23, 16p12, 18p11, and 20q13, the locations on 1q31, 2p21, 9p24, 9q31, 10q26, 12q23, and 16p12 have been reported in previous genome scans (Weeks et al. 2000, 2001; Majewski et al. 2003; Schick et al. 2003; Schmidt et al. 2003; Seddon et al. 2003). Family-by-family analysis (fig. 5) confirms the presence of these multiple loci and has uncovered signals on other chromosomes (e.g., 4q, 7p, 13p, and 17q) that may contribute to ARMD pathogenesis. The loci on chromosomes 4q and 17q have been described by other groups (Weeks et al. 2000, 2001; Majewski et al. 2003), but the other two are original reports. In general, our analysis has captured most of the previous linkage signals in addition to discovering new loci. We attribute our ability to identify novel signals and to cross-validate previously documented linkage to the use of a quantitative system with all levels of phenotypic severity, as opposed to a binary phenotype.

Thus, cross-validated loci on chromosomes 1q31, 9p24, 9q31, 10q26, 12q23, 16p12 and 17q25 are prob-

ably associated with advanced forms of the disease, because these loci were primarily identified through affected sib pair analysis. Our locus on chromosome 15q may predispose to drusen formation because it is present in both our genome scans. As described in the introduction, the previous genome scan for ARMD was based on milder forms of the disorder since the genotyped Beaver Dam sample was ascertained from a larger community-based sample which represented all levels of severity (Schick et al. 2003). At this juncture the observations pertaining to specific phenotypes driving particular linkage signals are merely speculative. Specific information on phenotypic diversity from other studies has not emerged to develop better-formulated hypotheses.

The proportion of families linked to 1q31 is disputed to range between 7–15% (Majewski et al. 2003) and 40% (Weeks et al. 2001). Our data support fewer families being linked to 1q31, although any estimate is subject to ascertainment bias. Further, not each family contributes equally to the linkage signal, and weak but pervasive modifier effects at the 1q31 locus cannot be presently eliminated.

Our family-by-family analysis has implications for the use of subsets or covariate analysis to enrich samples to detect weaker linkage signals. While these methods are useful to enhance linkage signals by reducing heterogeneity, they may unwittingly exclude particular epistatic interactions that are important in the etiology of the disease. These types of assumptions would have the greatest impact for diseases that are truly oligogenic in nature, as is ARMD. Contingent on the availability of extended families, we present an exploratory method that uses family-specific sib-pair allele sharing to assess which families contribute to the linkage signals at a particular locus. This method makes no assumption about the specific genetic model at any locus, and so may be more appropriate than assessing the heterogeneity fraction in a model-based analysis to determine the identity of linked families and the signal strength of this linkage in any given family. For example, at 10q26, two families, 454 and 460, contribute heavily to the linkage signal ($P < .0001$ per family), although at least 5 or 6 others demonstrate weak linkage (fig. 5). The discovery of these "strongly linked" families can now drive identification of haplotypes and mutations by use of more established methods.

One limitation of the above method is that the family-specific analysis can only be reliably conducted on extended families, which are seldom collected for multifactorial diseases. Other weaknesses of this method include the use of $-\log_{10} P$ value (pP) as a direct measure of the linkage signal strength in each family without appropriate adjustment for family size. Since, for LOD >0.5, the quantity pP is virtually linear in LOD (when only 1 df is involved) and the LOD is proportional to

the number of informative sib pairs per family, pP/(family size) may provide a better comparative measure. Thus, after adjustment for family size, smaller families will be weighted appropriately for the corresponding reduction in linkage evidence, but reliable exclusion of linkage may remain problematic for these families. This is an area that needs further theoretical investigation.

Finally, because of the combinatorial possibilities involving >10 loci, the phenotype-genotype correlations will not be easy to establish for ARMD, even if mutations are identified in some positional candidates. These difficulties will also follow when meta-analyses are proposed to boost weak linkage signals in multiple data sets. Conversely, linkage evidence in a single family led to identification of a putative candidate locus for ARMD1, namely hemicentin-1. Our family-by-family analysis and data published by other groups (Majewski et al. 2003; Schmidt et al. 2003) suggests that other such families exist for ARMD that may aid in positional cloning of these loci. We anticipate that the cloning of these loci will lead to important biological information on the RPE and its pathophysiology, which will help in constructing hypotheses on phenotype-genotype correlations for this complex disease.

In summary, our results suggest that the etiology of ARMD is multifactorial. Significant progress has been made by our group in identifying a major locus for ARMD pathophysiology on 15q and in confirming linkage reports at several other loci. We are also able to provide supporting evidence for hemicentin-1 as the ARMD1 locus by use of SNP analysis. In the future, we hope to be able to delineate the role of candidate genes on ARMD at other loci, including 15q, and to construct models for these genes that include their functional characteristics.

Acknowledgments

Electronic-Database Information

Accession numbers and URLs for data presented herein are as follows:

Ensembl Genome Browser, http://www.ensembl.org/ (hemicentin-1 transcript ID ENSG00000143341)

Marshfield Center for Medical Genetics, http://research.marshfieldclinic.org/genetics/

Online Mendelian Inheritance of Man (OMIM), http://www.ncbi.nlm.nih.gov/Omim/ (for EFEMP1)

References

Anonymous (2001) A randomized, placebo-controlled, clinical trial of high-dose supplementation with vitamins C and E, beta carotene, and zinc for age-related macular degeneration and vision loss. AREDS report no 8. Arch Ophthalmol 119: 1417–1436

Anonymous (2002) The effect of five-year zinc supplementation on serum zinc, serum cholesterol and hematocrit in persons randomly assigned to treatment group in the age-related eye disease study. AREDS Report No 7. J Nutr 132: 697–702

Allikmets R (2000) Further evidence for an association of ABCR alleles with age-related macular degeneration. The International ABCR Screening Consortium. Am J Hum Genet 67:487–491

Allikmets R, Shroyer NF, Singh N, Seddon JM, Lewis RA, Bernstein PS, Peiffer A, Zabriskie NA, Li Y, Hutchinson A, Dean M, Lupski JR, Leppert M (1997a) Mutation of the Stargardt disease gene (ABCR) in age-related macular degeneration. Science 277:1805–1807

Allikmets R, Singh N, Sun H, Shroyer NF, Hutchinson A, Chidambaram A, Gerrard B, Baird L, Stauffer D, Peiffer A, Rattner A, Smallwood P, Li Y, Anderson KL, Lewis RA, Nathans J, Leppert M, Dean M, Lupski JR (1997b) A photoreceptor cell-specific ATP-binding transporter gene (ABCR) is mutated in recessive Stargardt macular dystrophy. Nat Genet 15:236–246

Attebo K, Mitchell P, Smith W (1996) Visual acuity and the causes of visual loss in Australia. The Blue Mountains Eye Study. Ophthalmology 103:357–364

Balatsoukas DD, Sioulis C, Parisi A, Millar GT (1995) Visual handicap in south-east Scotland. J R Coll Surg Edin 40:49–51

Bernstein PS, Leppert M, Singh N, Dean M, Lewis RA, Lupski JR, Allikmets R, Seddon JM (2002) Genotype-phenotype analysis of ABCR variants in macular degeneration probands and siblings. Invest Ophthalmol Vis Sci 43:466–473

Bird AC, Bressler NM, Bressler SB, Chisholm IH, Coscas G, Davis MD, de Jong PT, Klaver CC, Klein BE, Klein R, Mitchell P, Sarks SH, Soubrane G, Taylor HR, Vingerling JR (1995) An international classification and grading system for age-related maculopathy and age-related macular degeneration. The International ARM Epidemiological Study Group. Surv Ophthalmol 39:367–374

Box G, Cox D (1964) An analysis of transformations (with discussions). J R Stat Soc B 26:211–254

Bressler NM (2002) Early detection and treatment of neovascular age-related macular degeneration. J Am Board Fam Pract 15:142–152

Buch H, Vinding T, La Cour M, Nielsen NV (2001) The prevalence and causes of bilateral and unilateral blindness in an elderly urban Danish population. The Copenhagen City Eye Study. Acta Ophthalmol Scand 79:441–449

Cordell HJ (2001) Sample size requirements to control for

stochastic variation in magnitude and location of allele-sharing linkage statistics in affected sibling pairs. Ann Hum Genet 65:491–502

Cruickshanks KJ, Klein R, Klein BE (1993) Sunlight and age-related macular degeneration. The Beaver Dam Eye Study. Arch Ophthalmol 111:514–518

De La Paz MA, Pericak-Vance MA, Lennon F, Haines JL, Seddon JM (1997) Exclusion of TIMP3 as a candidate locus in age-related macular degeneration. Invest Ophthalmol Vis Sci 38:1060–1065

DeBlack SS (2003) Cigarette smoking as a risk factor for cataract and age-related macular degeneration: a review of the literature. Optometry 74:99–110

Elston RC, Buxbaum S, Jacobs KB, Olson JM (2000) Haseman and Elston revisited. Genet Epidemiol 19:1–17

Evans J, Wormald R (1996) Is the incidence of registrable age-related macular degeneration increasing? Br J Ophthalmol 80:9–14

Fulker DW, Cherny SS, Sham PC, Hewitt JK (1999) Combined linkage and association sib-pair analysis for quantitative traits. Am J Hum Genet 64:259–267

Gorin MB (2001) The ABCA4 gene and age-related macular degeneration: innocence or guilt by association. Arch Ophthalmol 119:752–753

Guymer RH, Heon E, Lotery AJ, Munier FL, Schorderet DF, Baird PN, McNeil RJ, Haines H, Sheffield VC, Stone EM (2001) Variation of codons 1961 and 2177 of the Stargardt disease gene is not associated with age-related macular degeneration. Arch Ophthalmol 119:745–751

Guymer RH, McNeil R, Cain M, Tomlin B, Allen PJ, Dip CL, Baird PN (2002) Analysis of the Arg345Trp disease-associated allele of the EFEMP1 gene in individuals with early onset drusen or familial age-related macular degeneration. Clin Experiment Ophthalmol 30:419–423

Hammond CJ, Webster AR, Snieder H, Bird AC, Gilbert CE, Spector TD (2002) Genetic influence on early age-related maculopathy: a twin study. Ophthalmology 109:730–736

Harvey PT (2003) Common eye diseases of elderly people: identifying and treating causes of vision loss. Gerontology 49:1–11

Haseman JK, Elston RC (1972) The investigation of linkage between a quantitative trait and a marker locus. Behav Genet 2:3–19

Heiba IM, Elston RC, Klein BE, Klein R (1994) Sibling correlations and segregation analysis of age-related maculopathy: the Beaver Dam Eye Study. Genet Epidemiol 11:51–67

Hunt DW, Margaron P (2003) Status of therapies in development for the treatment of age-related macular degeneration. IDrugs 6:464–469

Jacques PF (1999) The potential preventive effects of vitamins for cataract and age-related macular degeneration. Int J Vitam Nutr Res 69:198–205

Jonasson F, Thordarson K (1987) Prevalence of ocular disease and blindness in a rural area in the eastern region of Iceland during 1980 through 1984. Acta Ophthalmol Suppl 182:40–43

Keverline MR, Mah TS, Keverline PO, Gorin MB (1998) A practice-based survey of familial age-related maculopathy. Ophthalmic Genet 19:19–26

Klein BE, Klein R, Lee KE, Moore EL, Danforth L (2001*a*) Risk of incident age-related eye diseases in people with an affected sibling: The Beaver Dam Eye Study. Am J Epidemiol 154:207–211

Klein ML, Schultz DW, Edwards A, Matise TC, Rust K, Berselli CB, Trzupek K, Weleber RG, Ott J, Wirtz MK, Acott TS (1998*a*) Age-related macular degeneration: clinical features in a large family and linkage to chromosome 1q. Arch Ophthalmol 116:1082–1088

Klein R, Clegg L, Cooper LS, Hubbard LD, Klein BE, King WN, Folsom AR (1999) Prevalence of age-related maculopathy in the Atherosclerosis Risk in Communities Study. Arch Ophthalmol 117:1203–1210

Klein R, Davis MD, Magli YL, Klein BEK (1991*a*) Wisconsin Age-Related Maculopathy Grading System. Accession number PB91-184267/AS, National Technical Information Service, Springfield, VA

Klein R, Davis MD, Magli YL, Segal P, Klein BE, Hubbard L (1991*b*) The Wisconsin age-related maculopathy grading system. Ophthalmology 98:1128–1134

Klein R, Klein BE, Jensen SC, Meuer SM (1997) The five-year incidence and progression of age-related maculopathy: the Beaver Dam Eye Study. Ophthalmology 104:7–21

Klein R, Klein BE, Lee KE, Cruickshanks KJ, Chappell RJ (2001*b*) Changes in visual acuity in a population over a 10-year period: The Beaver Dam Eye Study. Ophthalmology 108:1757–1766

Klein R, Klein BE, Linton KL (1992) Prevalence of age-related maculopathy. The Beaver Dam Eye Study. Ophthalmology 99:933–943

Klein R, Klein BE, Linton KL, De Mets DL (1991*c*) The Beaver Dam Eye Study: visual acuity. Ophthalmology 98:1310–1315

——— (1993) The Beaver Dam Eye Study: the relation of age-related maculopathy to smoking. Am J Epidemiol 137:190–200

Klein R, Klein BE, Moss SE (1998*b*) Relation of smoking to the incidence of age-related maculopathy: The Beaver Dam Eye Study. Am J Epidemiol 147:103–110

Klein R, Klein BE, Tomany SC, Meuer SM, Huang GH (2002*a*) Ten-year incidence and progression of age-related maculopathy: The Beaver Dam eye study. Ophthalmology 109:1767–1779

Klein R, Klein BE, Tomany SC, Moss SE (2002*b*) Ten-year incidence of age-related maculopathy and smoking and drinking: the Beaver Dam Eye Study. Am J Epidemiol 156:589–598

Klein R, Klein BEK (1991) Beaver Dam Eye Study: manual of operations. Accession number PB91-149823, National Technical Information Service, Springfield, VA

Klein R, Klein BEK (1995) Beaver Dam Eye Study II: manual of operations. Accession number PB95-273827, National Technical Information Service, Springfield, VA

Lander E, Kruglyak L (1995) Genetic dissection of complex traits: guidelines for interpreting and reporting linkage results. Nat Genet 11:241–247

Majewski J, Schultz DW, Weleber RG, Schain MB, Edwards AO, Matise TC, Acott TS, Ott J, Klein ML (2003) Age-related macular degeneration—a genome scan in extended families. Am J Hum Genet 73:540–550

Mares-Perlman JA, Klein R, Klein BE, Greger JL, Brady WE,

Palta M, Ritter LL (1996) Association of zinc and anti-oxidant nutrients with age-related maculopathy. Arch Ophthalmol 114:991–997

Marmorstein LY, Munier FL, Arsenijevic Y, Schorderet DF, McLaughlin PJ, Chung D, Traboulsi E, Marmorstein AD (2002) Aberrant accumulation of EFEMP1 underlies drusen formation in Malattia Leventinese and age-related macular degeneration. Proc Natl Acad Sci USA 99:13067–13072

Miller SA, Dykes DD, Polesky HF (1988) A simple salting out procedure for extracting DNA from human nucleated cells. Nucleic Acids Res 16:1215

Mittra RA (2003) New treatments for age-related macular degeneration. Minn Med 86:40–46

Olson JM (1999) Relationship estimation by Markov-process models in a sib-pair linkage study. Am J Hum Genet 64: 1464–1472

Rivera A, White K, Stohr H, Steiner K, Hemmrich N, Grimm T, Jurklies B, Lorenz B, Scholl HP, Apfelstedt-Sylla E, Weber BH (2000) A comprehensive survey of sequence variation in the ABCA4 (ABCR) gene in Stargardt disease and age-related macular degeneration. Am J Hum Genet 67:800–813

Schick JH, Iyengar SK, Klein BE, Klein R, Reading K, Liptak R, Millard C, Lee KE, Tomany SC, Moore EL, Fijal BA, Elston RC (2003) A whole-genome screen of a quantitative trait of age-related maculopathy in sibships from the beaver dam eye study. Am J Hum Genet 72:1412–1424

Schmidt S, Scott WK, Postel EA, Agarwal A, De La Paz M, Gilbert JR, Weeks DE, Haines JL, Gorin M, Pericak-Vance MA (2003) Genome screen and follow-up analysis on AMD multiplex families. Paper presented at Association for Research in Vision and Ophthalmology Meeting, Fort Lauderdale, FL, May 5–10

Schultz DW, Humpert AJ, Luzier CW, Persun V, Schain M, Weleber MG, Acott TS, Klein ML (2003) Evidence that FIBL-6 is the ARMD1 gene. Paper presented at Association for Research in Vision and Ophthalmology Meeting, Fort Lauderdale, FL, May 5–10

Seddon JM, Ajani UA, Sperduto RD, Hiller R, Blair N, Burton TC, Farber MD, Gragoudas ES, Haller J, Miller DT, Yannuzzi LA, Willett W (1994) Dietary carotenoids, vitamins A, C, and E, and advanced age-related macular degeneration. Eye Disease Case-Control Study Group. JAMA 272: 1413–1420

Seddon JM, Book K, Chong S, Cote J, Santangelo SL (2003) A genome wide scan for age related macular degeneration. Paper presented at Association for Research in Vision and Ophthalmology Meeting, Fort Lauderdale, FL, May 5–10

Shete S, Jacobs KB, Elston RC (2003) Adding further power to the Haseman and Elston method for detecting linkage in larger sibships: weighting sums and differences. Hum Hered 55:79–85

Stone EM, Lotery AJ, Munier FL, Heon E, Piguet B, Guymer RH, Vandenburgh K, Cousin P, Nishimura D, Swiderski RE, Silvestri G, Mackey DA, Hageman GS, Bird AC, Sheffield VC, Schorderet DF (1999) A single EFEMP1 mutation associated with both Malattia Leventinese and Doyne honeycomb retinal dystrophy. Nat Genet 22:199–202

Stone EM, Sheffield VC, Hageman GS (2001) Molecular genetics of age-related macular degeneration. Hum Mol Genet 10:2285–2292

Timpl R, Sasaki T, Kostka G, Chu ML (2003) Fibulins: a versatile family of extracellular matrix proteins. Nat Rev Mol Cell Biol 4:479–489

Tiwari HK, Elston RC (1997) Linkage of multilocus components of variance to polymorphic markers. Ann Hum Genet 61:253–261

VandenLangenberg GM, Mares-Perlman JA, Klein R, Klein BE, Brady WE, Palta M (1998) Associations between anti-oxidant and zinc intake and the 5-year incidence of early age-related maculopathy in the Beaver Dam Eye Study. Am J Epidemiol 148:204–214

VanNewkirk MR, Weih L, McCarty CA, Stanislavsky YL, Keeffe JE, Taylor HR (2000) Visual impairment and eye diseases in elderly institutionalized Australians. Ophthalmology 107:2203–2208

VanNewkirk MR, Weih L, McCarty CA, Taylor HR (2001) Cause-specific prevalence of bilateral visual impairment in Victoria, Australia: the Visual Impairment Project. Ophthalmology 108:960–967

Vinding T (1990) Visual impairment of age-related macular degeneration: an epidemiological study of 1000 aged individuals. Acta Ophthalmol (Copenh) 68:162–167

Vogel BE, Hedgecock EM (2001) Hemicentin, a conserved extracellular member of the immunoglobulin superfamily, organizes epithelial and other cell attachments into oriented line-shaped junctions. Development 128:883–894

Weeks DE, Conley YP, Mah TS, Paul TO, Morse L, Ngo-Chang J, Dailey JP, Ferrell RE, Gorin MB (2000) A full genome scan for age-related maculopathy. Hum Mol Genet 9:1329–1349

Weeks DE, Conley YP, Tsai HJ, Mah TS, Rosenfeld PJ, Paul TO, Eller AW, Morse LS, Dailey JP, Ferrell RE, Gorin MB (2001) Age-related maculopathy: an expanded genome-wide scan with evidence of susceptibility loci within the 1q31 and 17q25 regions. Am J Ophthalmol 132:682–692

Wilson AF, Elston RC (1993) Statistical validity of the Haseman-Elston sib-pair test in small samples. Genet Epidemiol 10:593–598

Wilson AF, Elston RC, Tran LD, Siervogel RM (1991) Use of the robust sib-pair method to screen for single-locus, multiple-locus, and pleiotropic effects: application to traits related to hypertension. Am J Hum Genet 48:862–872

Wiltshire S, Cardon LR, McCarthy MI (2002) Evaluating the results of genomewide linkage scans of complex traits by locus counting. Am J Hum Genet 71:1175–1182

Yoshida A, Yoshida M, Yoshida S, Shiose S, Hiroishi G, Ishibashi T (2000) Familial cases with age-related macular degeneration. Jpn J Ophthalmol 44:290–295